RELEASE NOTICE

TO: DSN Document 810-5 Distribution July 1, 1998

FROM: R. W. Sniffin, Editor

SUBJECT: Update of DSN Document 810-5

Please make the changes listed below in your copy of DSN Document 810-5, Volume I. In addition to this mail distribution, the revised modules are available in pdf form (requires Adobe Acrobat™) from our web server, **http://deepspace1.jpl.nasa.gov/810-5/** .

I would like to encourage you to take advantage of the electronic distribution of this document. I will notify those on our distribution list who have supplied me with an e-mail address and indicated they are willing to print out the pdfs at their location at the time I send the revision to be printed. This is at least two weeks before it is ready to be distributed by mail. If you think that such an approach would be beneficial to you, please notify me and I will modify our distribution list. My e-mail address is **Robert.W.Sniffin@jpl.nasa.gov** .

Module ID	New Status	Procedural Instructions	Remarks
TRK-21	New Module	Insert new TRK-21 tab and module in front of existing TRK-30 tab.	Provides information on Doppler tracking performance when using the Block V digital receivers.

Table of Contents as of July 1, 1998

(Replaces Table of Contents as of July 15, 1997)

Table of Contents as of July 1, 1998 (Continued)

DSN/Flight Project
Interface Design

TRK-21
DSN Tracking System,
Block-V Receiver Doppler

July 1, 1998

Prepared by:

P. W. Kinman

Approved by:

E. J. Christensen

Released by:

K. J. Schoeni
DSN Document Release

Change Log

Change Number	Date	Affected Pages
Initial Issue	7/1/98	All

Contents

Appendices

Illustrations

Tables

1. Introduction

1.1 Purpose

This module defines the Doppler data types and identifies the performance parameters for Doppler measurement with the Block-V Receiver.

1.2 Scope

The scope of this module is limited to those features of the Block-V Receiver that relate to the measurement and reporting of the Doppler effect.

2. General Information

A two-way (or three-way) coherent Doppler measurement requires information about both the uplink and downlink carrier phase (Reference 1). The Metric Data Assembly (MDA) keeps a record of the tuning history of the exciter from which the exciter phase can be calculated. Furthermore, the Block-V Receiver reports sampled downlink carrier phase to the MDA via the Signal Processing Center (SPC) Local Area Network (LAN). Thus, the principal data needed to compute the Doppler effect are available at the MDA. Figure 1 illustrates two-way Doppler measurement with the Block-V Receiver. Channel frequencies are listed in TRK-50.

One important advantage of the Block-V Receiver over the earlier analog receivers, the Block-III and Block-IV, is evident from Figure 1. Two-way Doppler measurement with the Block-V Receiver does not utilize any real-time, analog signal connections between the receiver and exciter. This means greater flexibility in configuring station equipment. Furthermore, three-way Doppler measurement is essentially the same as two-way. The only difference is that two MDAs are required: one at the transmitting station to record uplink carrier phase and one at the receiving station to record downlink carrier phase.

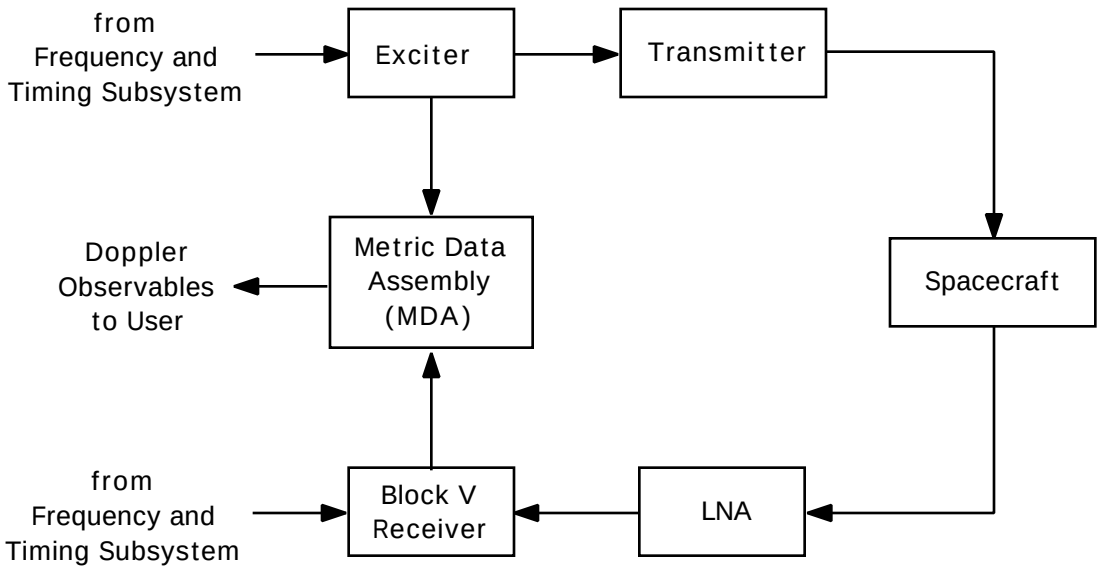

Figure 1. Two-Way Doppler Measurement With Block-V Receiver

Figure 2 shows the signal path at the receiving end for a Doppler measurement with the Block-V Receiver, including the main architectural features of the receiver. At the front of the receiver are multiple stages of analog downconversion. The hardware used within these stages depends on the band in which the downlink is operating. The local oscillators remain at a constant setting for the duration of a tracking pass. The channel-select synthesizer is adjusted before the beginning of a pass to a frequency appropriate for the channel (within the band) of the incoming downlink signal; during the pass the frequency of this synthesizer remains constant. The anti-aliasing filter is a necessary precursor to sampling, and the Automatic Gain Control (AGC) is a necessary precursor to quantization. The remainder of the signal processing in the receiver is done digitally (Reference 2); this includes carrier synchronization and, if necessary, Doppler compensation. The downlink carrier phase information that is needed for a Doppler measurement is passed to the MDA via the SPC LAN.

The Block-V Receiver differs markedly from the earlier analog receivers, the Block III and Block IV, in a number of important respects. The Block-V Receiver can track either a residual carrier or a suppressed carrier downlink and provide the accurate carrier phase counts needed for a Doppler measurement. Suppressed-carrier tracking is accomplished with a Costas loop (Reference 3). Also, the carrier loop bandwidth of the Block-V Receiver can be freely chosen by the user from a continuum of possible values, and this bandwidth can be changed during a tracking pass without losing phase-lock. This flexibility in the selection and change of carrier loop bandwidth obviates the kind of coarse bandwidth adaptivity that was built into the analog receivers. (The Block-III and Block-IV Receivers were designed with bandpass limiters preceding the final carrier phase detector, causing carrier loop bandwidth to vary with signal level.)

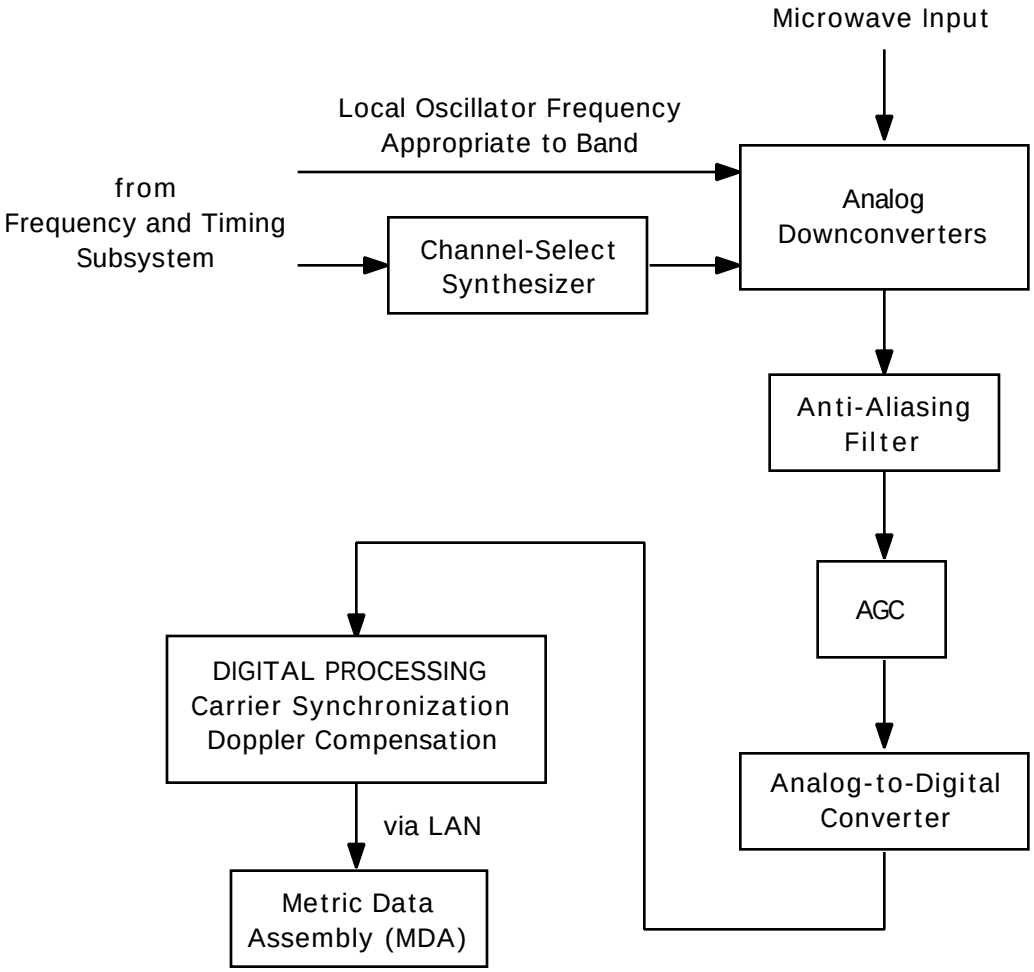

Figure 2. Doppler Measurement With the Block-V Receiver

The Block-V Receiver offers the prospect of using very small carrier loop bandwidths. This is made possible by two elements of this receiver's design. The carrier loop is closed at an intermediate-frequency stage, which reduces the amount of frequency multiplication required within the loop; and the loop closure is digital, which makes the loop parameters numeric. These design elements ensure loop stability that is much superior to that of the analog receivers. As a result, the narrowest carrier loop bandwidth that can be used with the Block-V Receiver is limited only by the inherent stability of the incoming carrier and by the amount of uncompensated Doppler dynamics present.

2.1 Doppler Data Types

The data from the MDA are usually formatted and packaged by a Radio-Metric Data Conditioner (RMDC) before being delivered to the flight project. The format of the data as delivered by the RMDC is often mission-specific and will not be discussed here. This section discusses two methods by which data are reported by the MDA to the RMDCs and how Doppler can be derived from this data.

The MDA has traditionally reported Doppler data in accordance with the TRK-2-15A data interface (Reference 4). This format provides data as a continuous cycle count, including fractions, of the 1 MHz Biased Doppler observable. This data type also includes uplink ramp information from which uplink phase can be calculated. A new data format is being introduced which contains the actual uplink and downlink phase as reported by the exciter and receiver. Both formats are summarized below.

2.1.1 Doppler Using TRK-2-15A Data

The TRK-2-15A data type is identical to what has been provided by the MDA at S-band uplink stations when no uplink signal is being transmitted (one-way or three-way Doppler). This compatibility is advantageous to users with older software. Ten values are reported each second. The ten reported values correspond to raw downlink carrier phase counts that are spaced uniformly 0.1 second apart, and every tenth value corresponds to the raw phase count at the one pulse-per-second epoch as defined by the station reference. The TRK-2-15A reported values for downlink phase equal

$$\frac{n}{10}\left(96\,G_R\,f_{ref} + f_b\right) - \varphi_d\left(\frac{n}{10}\right) \tag{1}$$

where

n = integer count of reported values

$\varphi_d(t)$ = raw downlink carrier phase count referenced to the sky frequency, cycles

G_R = 240/221, 880/221, or 3344/221 depending on whether received frequency is in the S, X, or Ka-band

f_{ref} = reference frequency

f_b = Doppler bias: +1 MHz.

The reference frequency, f_{ref}, is calculated from the initial received sky frequency as part of the acquisition process and is nominally in the range of 21.1 to 22.2 MHz. The reported value does not change unless re-acquisition is required.

When using TRK-2-15A data, it is the responsibility of the user to calculate the uplink phase by integrating the frequency ramp data which is provided in the data format as a series of start times, start frequencies, and rate of change of frequency. The Doppler

frequency, if desired, can then be calculated from the downlink and uplink phase along with other factors such as the transponder ratio, uplink and downlink light-times, etc.

2.1.2 Doppler Using Uplink and Downlink Phase

The new Doppler data type is simply the sampled uplink and downlink carrier phase counts, referenced to the sky frequency. The sampling rate is variable with a maximum of ten samples per second. In the notation of the previous paragraph, the two observables at the maximum sampling rate are

$$\varphi_d\left(\frac{n}{10}\right) \text{ and } \varphi_u\left(\frac{n}{10}\right). \tag{2}$$

Doppler frequency, if desired, can be calculated directly from these observables and other factors by the same technique as used with TRK-2-15A data.

2.2 Carrier Tracking

The Block-V Receiver can be configured to track either a residual carrier or a suppressed carrier, the latter with a Costas loop. In order to achieve good Doppler measurement performance, it is important to characterize the phase error in the carrier loop.

2.2.1 Carrier Loop Bandwidth

In this module, carrier loop bandwidth means the one-sided, noise-equivalent carrier loop bandwidth of the Block-V Receiver. It will be denoted B_L. The carrier loop bandwidth of the Block-V Receiver may be precisely selected from a continuum of possible values (over some range that is characterized by an upper and lower limit). Unlike the Block-III and Block-IV Receivers, the Block-V Receiver does not have a predetection bandpass limiter; thus, its carrier loop bandwidth does not vary with signal level. With the Block-V Receiver, the user may make a precise selection for B_L and that selection will continue to characterize the carrier loop even in the presence of a varying signal level. The user may choose to change B_L during a tracking pass and this can be implemented without losing phase-lock, assuming the change is not too large.

There are limits on the carrier loop bandwidth. B_L can be no larger than 200 Hz. The lower limit on B_L is determined by the phase noise on the downlink. In addition, when operating in the suppressed-carrier mode, B_L is subject to the following constraint.

$$B_L \le \frac{R_{SYM}}{20}, \quad \text{suppressed carrier,} \tag{3}$$

where R_{SYM} is the telemetry symbol rate.

In general, the value selected for B_L should be small in order to maximize the carrier loop signal-to-noise ratio. On the other hand, B_L must be large enough that neither of the following variables becomes too large: the static phase error due to Doppler dynamics, the contribution to carrier loop phase error variance due to phase noise on the downlink. The best

B_L to select will depend on circumstances. Often, it will be possible to select a B_L of less than 1 Hz. A larger value for B_L is necessary when there is significant uncertainty in the downlink Doppler dynamics, when the downlink is one-way (or two-way noncoherent) and originates with a less stable oscillator (such as an Auxiliary Oscillator), or when the sun-earth-probe angle is small (so that solar phase scintillations are present on the downlink).

The user may select either a type 2 or type 3 carrier loop. Both loop types are perfect, meaning that the loop filter implements a true accumulation.

2.2.2 Static Phase Error in the Carrier Loop

The Block-V Receiver, with either a type 2 or type 3 loop, has a very large tracking range; even a Doppler offset of several megahertz can be tracked. With a finite Doppler rate, however, there will be a static phase error in a type 2 loop.

Table 1 shows the static phase error in the carrier loop of the Block-V Receiver that results from various Doppler dynamics for several different loops. These equations are based on the work reported in Reference 5. The Doppler dynamics are here defined by the parameters α and β.

$$\alpha = \text{Doppler Rate (Hz/s)} \tag{4}$$

$$\beta = \text{Doppler Acceleration (Hz/s}^2\text{)} \tag{5}$$

In the presence of a persistent Doppler acceleration, a type 2 loop will periodically slip cycles.

The equations of Table 1 are valid for either residual-carrier or suppressed-carrier (Costas loop) operation of the Block-V Receiver. These equations are exactly the same as those appearing in Appendix C of module TLM-21.

2.2.3 Carrier Phase Error Variance

When the spacecraft is tracked in a two-way or three-way coherent mode, the carrier phase error variance σ_φ^2 in the Block-V Receiver is given by

$$\sigma_\varphi^2 = \frac{1}{\rho_L} + \frac{G^2\left(B_{TR} - B_L\right)}{P_C / N_0\big|_{U/L}} + \sigma_S^2 \tag{6}$$

where

G = transponding ratio

$P_C / N_0\big|_{U/L}$ = uplink carrier power to noise spectral density ratio, Hz

B_{TR} = one-sided, noise-equivalent, transponder carrier loop bandwidth, Hz

Table 1. Static Phase Error (rad) for Block-V Receiver

Loop	Constant Range-Rate $\left(\text{Constant Doppler Offset}\right)$	Constant Derivative of Range-Rate $\left(\text{Constant Doppler Rate}\right)$	Constant Second Derivative of Range-Rate $\left(\text{Constant Doppler Acceleration}\right)$
type 2, standard underdamped	0	$\frac{9\pi}{16B_L^2}\ \alpha$	$\left(\frac{9\pi\beta}{16B_L^2}\right)\dot{\alpha}t - \frac{27\pi\beta}{64B_L^3}$
type 2, supercritically damped	0	$\frac{25\pi}{32B_L^2}\ \alpha$	$\left(\frac{25\pi\beta}{32B_L^2}\right)\dot{\alpha}t - \frac{125\pi\beta}{128B_L^3}$
type 3, standard underdamped	0	0	$\frac{12167\pi}{8000B_L^3}\ \beta$
type 3, supercritically damped	0	0	$\frac{35937\pi}{16384B_L^3}\ \beta$

ρ_L = downlink carrier loop signal-to-noise ratio

σ_S^2 = contribution to carrier loop phase error variance due to solar phase scintillations, rad^2 (see Appendix A).

When tracking a residual carrier, the carrier loop signal-to-noise ratio is

$$\rho_L = \left.\frac{P_C}{N_0}\right|_{D/L} \frac{1}{B_L} \tag{7}$$

where

$\left.P_C/N_0\right|_{D/L}$ = downlink carrier power to noise spectral density ratio, Hz.

There is an additional loss to the carrier loop signal-to-noise ratio when tracking a residual carrier with non-return-to-zero symbols in the absence of a subcarrier. This loss is due to the presence of data sidebands overlaying the residual carrier in the frequency domain and therefore increasing the effective noise level for carrier synchronization. ρ_L, in this case, must be calculated as (Reference 6)

$$\rho_L = \left.\frac{P_C}{N_0}\right|_{D/L} \quad \frac{1}{B_L} \quad \frac{1}{1 + 2\,E_S/N_0} \tag{8}$$

where

E_S/N_0 = energy per symbol to noise spectral density ratio.

When tracking a suppressed carrier, the carrier loop signal-to-noise ratio is

$$\rho_L = \left.\frac{P_T}{N_0}\right|_{D/L} \quad \frac{S_L}{B_L} \tag{9}$$

where

$P_T/N_0|_{D/L}$ = downlink total signal power to noise spectral density ratio, Hz

S_L = squaring loss of the Costas loop (Reference 7),

$$S_L = \frac{2\,\frac{E_S}{N_0}}{1 + 2\,\frac{E_S}{N_0}}\,. \tag{10}$$

It is recommended that the following constraint on carrier phase error variance be observed.

$$\sigma_\varphi^2 \le \begin{cases} 0.10\,\text{rad}^2, & \text{residual carrier} \\ 0.02\,\text{rad}^2, & \text{suppressed carrier} \end{cases} \tag{11}$$

2.3 Carrier Power Measurement

When the downlink is residual-carrier, the Block-V Receiver provides an estimate of the downlink carrier power P_C. When the downlink is suppressed-carrier, the Block-V Receiver provides an estimate of the total downlink power P_T. This it does by first estimating $P_C/N_0|_{D/L}$ (with the algorithm described in Reference 8) or $P_T/N_0|_{D/L}$ (with the split-symbol moments algorithm described in Reference 9). An estimate of the noise spectral density N_0 comes from continual measurements made by a noise-adding radiometer. The Block-V Receiver then computes the absolute power P_C or P_T. The results are reported once per second.

2.4 Measurement Error for Two-(Three-)Way Coherent Doppler

This section summarizes the expected measurement errors for two-way coherent and three-way coherent Doppler. Each error is characterized here as a standard deviation of range-rate σ_v and is in units of velocity. To translate any of these errors to a standard deviation of frequency σ_f, the following equation can be used.

$$\sigma_f = \frac{2 f_c}{c} \sigma_v \tag{12}$$

where f_C is the downlink carrier frequency and c is the speed of light in vacuum.

Only errors in measuring the rate-of-change of the distance between phase centers of the antennas are considered in this section. There are other errors that must be considered in any navigation solution.

2.4.1 Error Due to Thermal Noise

The two-way or three-way coherent Doppler measurement error due to thermal noise is approximated by

$$\sigma_v = \frac{c}{2\sqrt{2}\pi f_c T} \sqrt{\frac{1}{\rho_L} + \frac{G^2 B_L}{P_C / N_0 \big|_{U/L}}} \tag{13}$$

where

T = the measurement integration time,

f_C = the downlink carrier frequency, and

c = the speed of light in vacuum.

The other parameters were defined in Section 2.2.3.

2.4.2 Error Due to Solar Phase Scintillations

When the sun-earth-probe angle is small and the spacecraft is beyond the sun, microwave carriers pick up phase scintillations in passing through the solar corona. There is a resulting contribution to Doppler measurement error. The magnitude of the effect is highly variable, depending on the activity of the sun. Equations (14) and (15), below, based on the work reported in Reference 10, offer a coarse estimate of the average solar contribution. It is valid for the Block-V Receiver tracking either a residual carrier or a suppressed carrier and for sun-earth-probe angles between 5° and 27°.

$$\sigma_v = \frac{0.73 c \sqrt{C_{band}} \left[\sin(\theta_{SEP})\right]^{-1.225}}{f_c T^{0.175}} \tag{14}$$

T is the measurement integration time in seconds, f_C is the downlink carrier frequency in hertz, c is the speed of light in vacuum (3.0×10^{11} mm/s), and ϑ_{SEP} is the sun-earth-probe angle. σ_v has the same units as c. The constant C_{band} depends on the uplink/downlink bands; it is given by

$$C_{band} = \begin{cases} 6.1 \times 10^{-5}, & \text{S-up/S-down} \\ 4.8 \times 10^{-4}, & \text{S-up/X-down} \\ 5.5 \times 10^{-6}, & \text{X-up/X-down} \\ 5.2 \times 10^{-5}, & \text{X-up/Ka-down} \end{cases} . \qquad (15)$$

Figure 3 shows σ_v as a function of sun-earth-probe angle for two-way or three-way Doppler measurement with an S-band uplink and an S-band downlink. The vertical axis is in units of mm/s. The three curves in that figure correspond to measurement integration times of 5, 60, and 1000 seconds. Figure 4 shows σ_v for an S-band uplink and an X-band downlink. Figure 5 shows σ_v for an X-band uplink and an X-band downlink. Figure 6 shows σ_v for an X-band uplink and a Ka-band downlink.

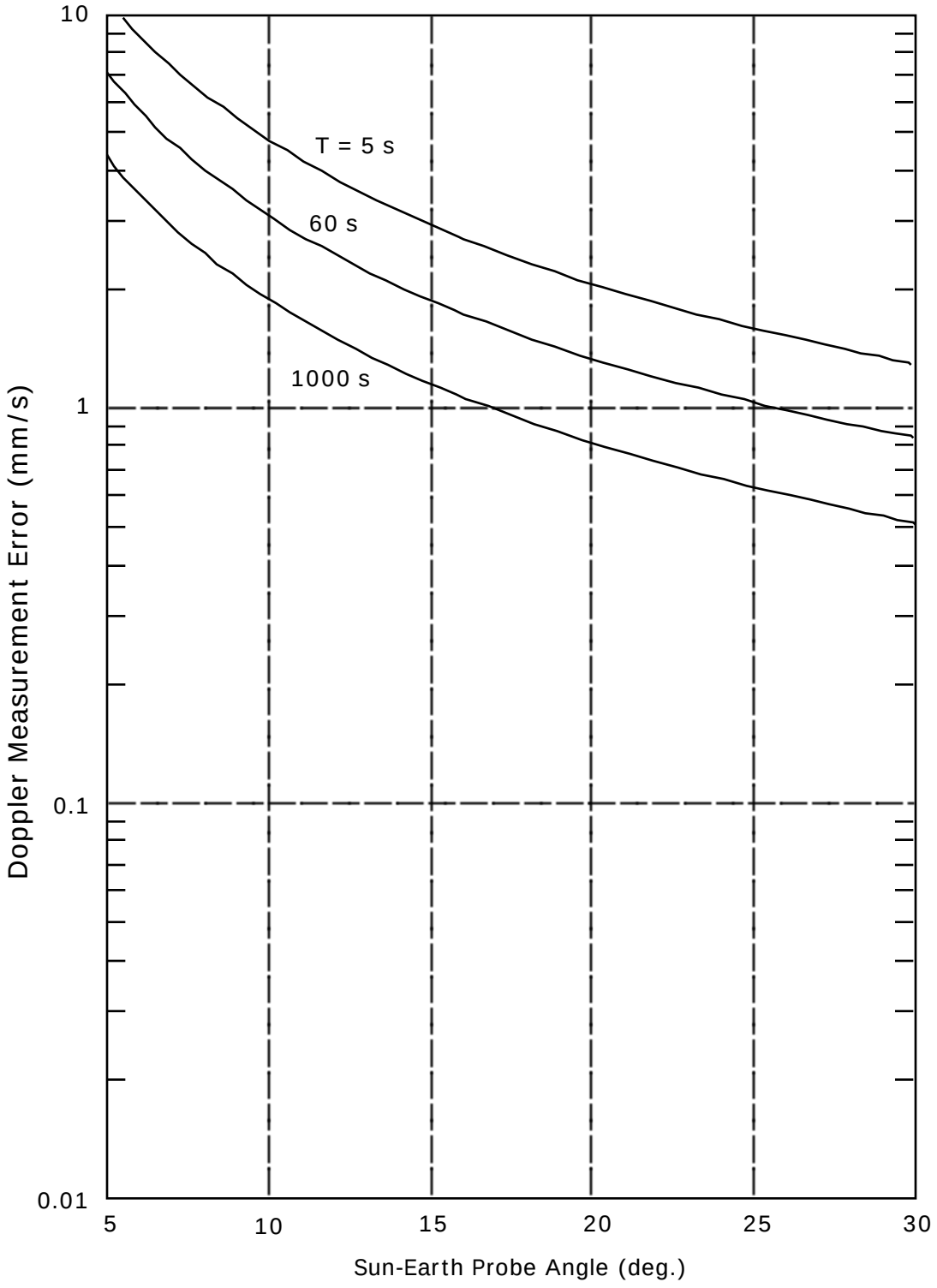

Figure 3: Doppler Measurement Error Due to Solar Phase Scintillation: S-Up/S-Down

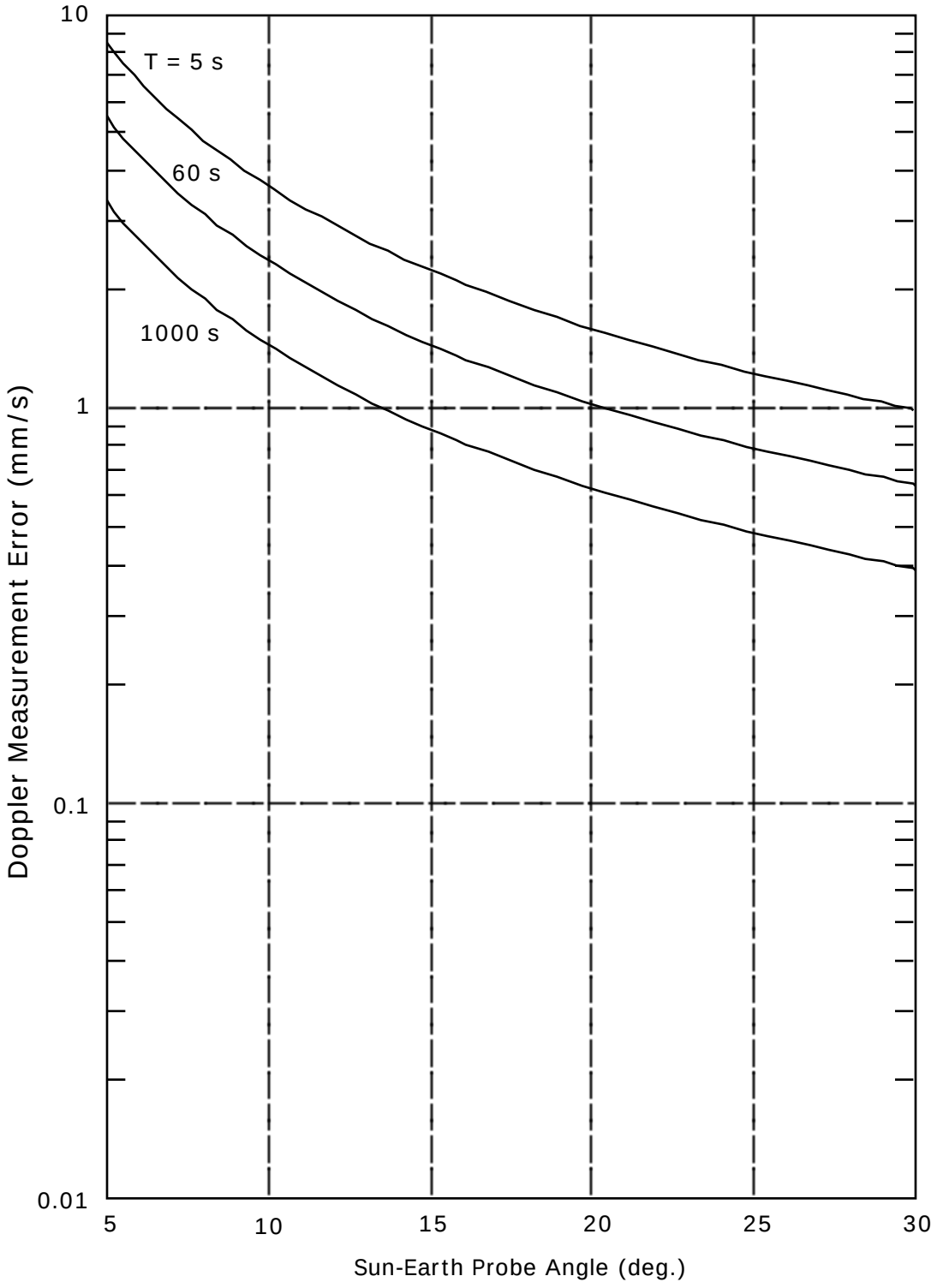

Figure 4: Doppler Measurement Error Due to Solar Phase Scintillation: S-Up/X-Down

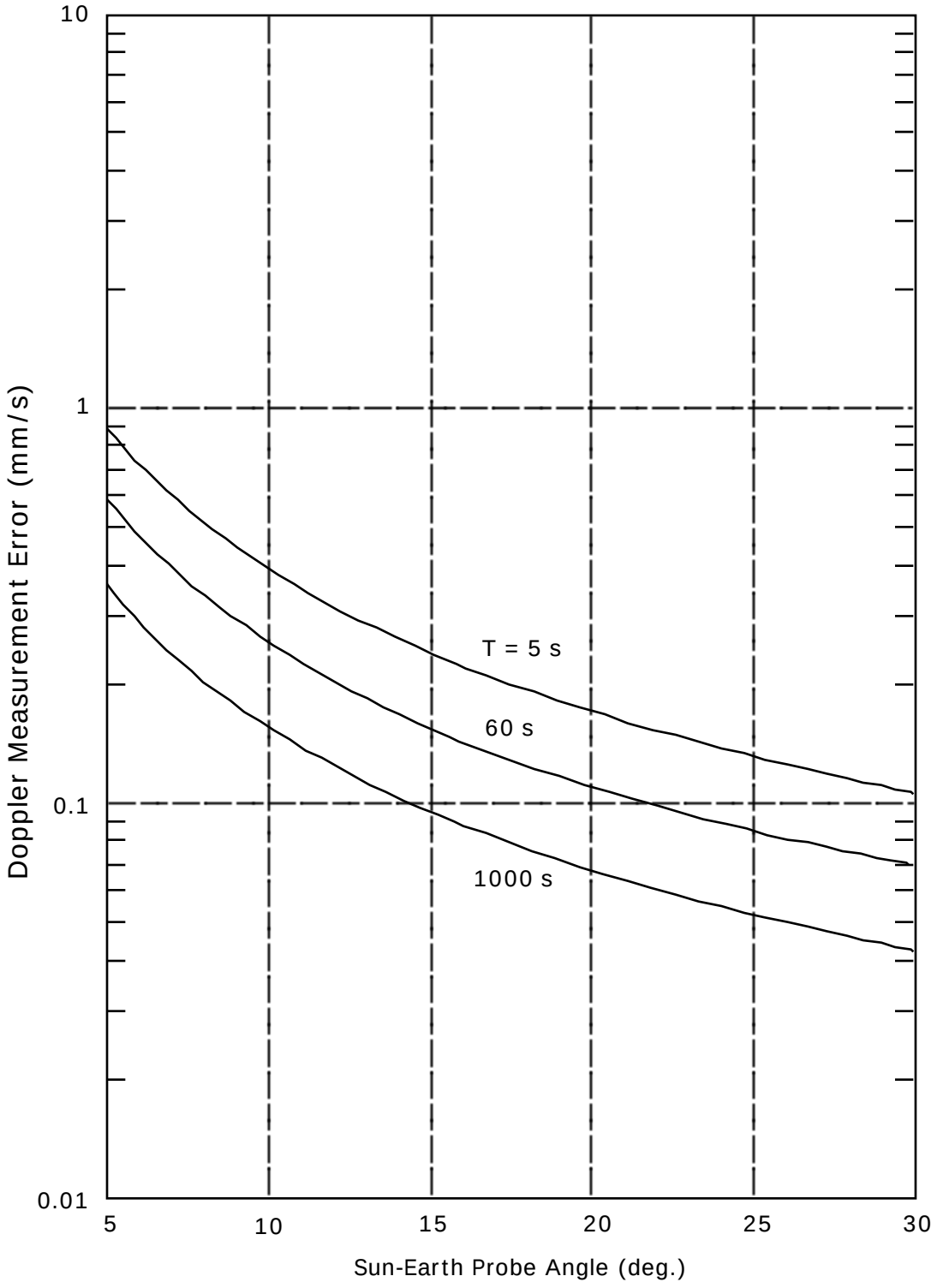

Figure 5: Doppler Measurement Error Due to Solar Phase Scintillation: X-Up/X-Down

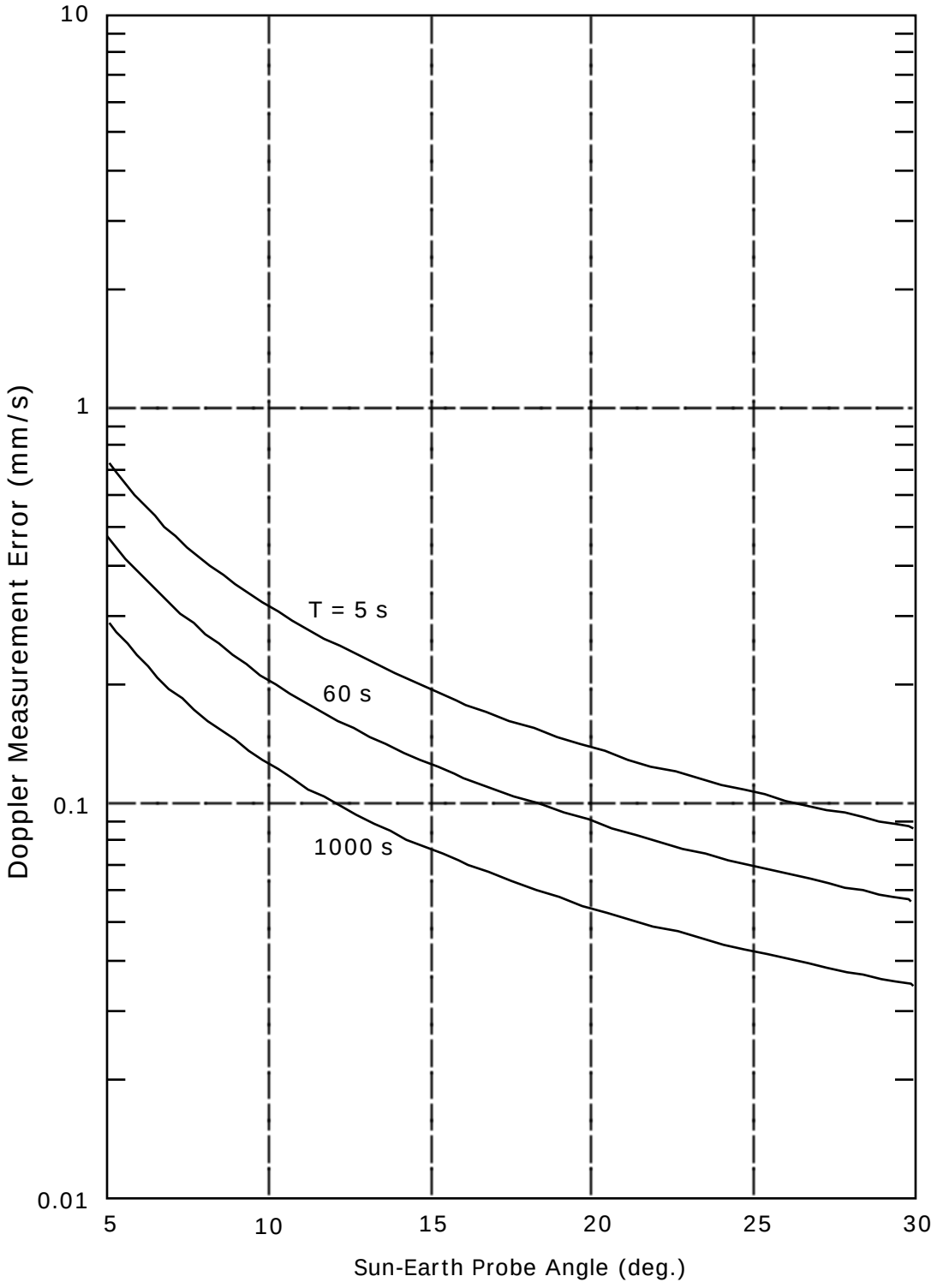

Figure 6: Doppler Measurement Error Due to Solar Phase Scintillation: X-Up/Ka-Down

Appendix A

Contribution of Solar Phase Scintillations to Carrier Phase Error Variance

Equation (A-1), below, based on the work reported in Reference 10, offers a coarse estimate of the average solar contribution, in units of rad^2 to carrier loop phase error variance. It is valid for the Block-V Receiver tracking either a residual carrier or a suppressed carrier and for sun-earth-probe angles between 5° and 27°.

$$\sigma_s^2 = \frac{C_{band}\ C_{loop}}{\left(\sin\theta_{SEP}\right)^{2.45}\ B_L^{1.65}}, \quad 5° \le \theta_{SEP} \le 27° \tag{A-1}$$

In Equation (A-1) ϑ_{SEP} is the sun-earth-probe angle and B_L is carrier loop bandwidth. C_{band} is a constant for a given set of operating bands. For two-way or three-way coherent operation,

$$C_{band} = \begin{cases} 6.1\times10^{-5}, & \text{S-up/S-down} \\ 4.8\times10^{-4}, & \text{S-up/X-down} \\ 5.5\times10^{-6}, & \text{X-up/X-down} \\ 5.2\times10^{-5}, & \text{X-up/Ka-down} \end{cases} \tag{A-2}$$

Equation (A-2) is the same as Equation (15).

C_{loop} is a constant for a given carrier loop.

$$C_{loop} = \begin{cases} 5.9, & \text{standard underdamped type 2 loop} \\ 5.0, & \text{supercritically damped type 2 loop} \\ 8.2, & \text{standard underdamped type 3 loop} \\ 6.7, & \text{supercritically damped type 3 loop} \end{cases} \tag{A-3}$$

Appendix B

References

1. P. W. Kinman, "Doppler Tracking of Planetary Spacecraft," *IEEE Transactions on Microwave Theory and Techniques*, Vol. 40, No. 6, pp. 1199-1204, June 1992.

2. J. B. Berner and K. M. Ware, "An Extremely Sensitive Digital Receiver for Deep Space Satellite Communications," *Eleventh Annual International Phoenix Conference on Computers and Communications*, pp. 577-584, Scottsdale, Arizona, April 1-3, 1992.

3. J. P. Costas, "Synchronous Communications," *Proceedings of the IRE*, Vol. 44, pp. 1713-1718, December 1956.

4. JPL Document 820-13, TRK-2-15A, *DSN Tracking System Interfaces, Metric Data Assembly Interface*.

5. S. A. Stephens and J. B. Thomas, "Controlled-Root Formulation for Digital Phase-Locked Loops," *IEEE Transactions on Aerospace and Electronic Systems*, Vol. 31, No. 1, pp. 78-95, January 1995.

6. J. Lesh, "Tracking Loop and Modulation Format Considerations for High Rate Telemetry," *DSN Progress Report 42-44*, pp. 117-124, April 15, 1978.

7. M. K. Simon and W. C. Lindsey, "Optimum Performance of Suppressed Carrier Receivers with Costas Loop Tracking," *IEEE Transactions on Communications*, Vol. COM-25, No. 2, pp. 215-227, February 1977.

8. A. Monk, "Carrier-to-Noise Power Estimation for the Block-V Receiver," *TDA Progress Report 42-106*, pp. 353-363, August 15, 1991.

9. S. Dolinar, "Exact Closed-Form Expressions for the Performance of the Split-Symbol Moments Estimator of Signal-to-Noise Ratio," *TDA Progress Report 42-100*, pp. 174-179, February 15, 1990.

10. R. Woo and J. W. Armstrong, "Spacecraft Radio Scattering Observations of the Power Spectrum of Electron Density Fluctuations in the Solar Wind," *Journal of Geophysical Research*, Vol. 84, No. A12, pp. 7288-7296, December 1, 1979.`